# On ISAC Performance with Full-Duplex FAS-assisted BS

Boyi Tang\*, Hao Xu<sup>†</sup>, Kai-Kit Wong\*<sup>||</sup>, Kaitao Meng\*, Ross Murch<sup>‡</sup> Chan-Byoung Chae<sup>§</sup> Yangyang Zhang<sup>¶</sup>
\*Department of Electronic and Electrical Engineering, University College London, London WC1E7JE, U.K.

<sup>†</sup>National Mobile Communications Research Laboratory, Southeast University, Nanjing 210096, China.

<sup>‡</sup>Department of Electronic and Computer Engineering and Institute for Advanced Study (IAS), Hong Kong
University of Science and Technology, Clear Water Bay, Hong Kong SAR, China.

School of Integrated Technology, Yonsei University, Seoul, 03722, Korea.

¶Kuang-Chi Science Limited, Hong Kong SAR, China.

Yonsei Frontier Laboratory, Yonsei University, Seoul, 03722, Korea.

E-mail: {boyi.tang.22, kai-kit.wong, kaitao.meng}@ucl.ac.uk; hao.xu@seu.edu.cn; eermurch@ust.hk; cbchae@yonsei.ac.kr; yangyang.zhang@kuang-chi.com

Abstract—This paper studies the integrated sensing and communication (ISAC) performance of a full-duplex network assisted by fluid antenna systems (FAS). The base station (BS) operates in full-duplex mode and employs planar FASs for both transmission and reception. It simultaneously communicates with a downlink user, an uplink user, and performs target sensing. Our objective is to maximize the overall communication rate while ensuring the sensing requirements. Due to the non-convex and intractable nature of the optimization problem, we first reformulate it using the fractional programming (FP) framework. Subsequently, we iteratively optimize the antenna positions of both transmit and receive FASs, the beamforming vectors, and the uplink transmit power. The antenna position optimization subproblems are converted into convex quadratically constrained quadratic programs (QCQPs) and solved via the successive convex approximation (SCA) method. Simulation results demonstrate that the FAS significantly outperforms traditional fixed-position antenna systems by achieving higher communication rates.

Index Terms—Fluid antenna system, ISAC, full-duplex, fractional programming, successive convex approximation (SCA).

# I. INTRODUCTION

The next generation of wireless technology, envisioned for the 2030s, is poised to transform communication systems by harnessing advanced artificial intelligence (AI), enhanced environmental sensing, and the convergence of diverse emerging technologies [1], [2]. Key targets for sixth generation (6G) include ultra-high connectivity with data rates reaching up to 1 terabit per second, spectral efficiency of up to 1000 bps/Hz, and ultra-low latency as low as 1 microsecond ( $\mu$ s) [3]. These breakthroughs will empower 6G networks to handle massive data volumes and support an unprecedented number of connected devices, paving the way for transformative applications such as immersive extended reality (IXR), hyper-intelligent cities, and remote healthcare services [4].

To enhance wireless communication, Wong *et al.* introduced the concept of the fluid antenna system (FAS) in [5]. Broadly, FAS refers to any antenna system that is flexible in both shape and position [6], [7]. Practical implementations of FAS include liquid-based antennas [8], pixel-reconfigurable antennas [9], and mechanically movable antennas [10]. By leveraging spatial degrees of freedom (DoF), FAS enables improved spatial

diversity using only a single radio frequency (RF) chain, thereby reducing the need for multiple antennas and RF chains [11], [12], [13]. In addition, FAS reduces the dependence on channel state information (CSI) at the transmitter for multiuser communication by exploiting the natural fading behavior of both desired and interfering signals, a principle that underpins fluid antenna multiple access (FAMA) [14], [15], [16].

Recent research on FAS has highlighted their potential to significantly enhance communication system performance. In [17], the diversity performance of FAS is analyzed under equally correlated Nakagami-m fading channels. Exact and asymptotic expressions for the outage probability in FAS-aided wireless powered communication systems are derived in [18]. Additionally, [19] explores the capability of FAS to address common challenges in the terahertz (THz) band. In the context of near-field communication, [20] investigates energy efficiency maximization by jointly optimizing the beamforming vector and antenna positions. Furthermore, [21] demonstrates how FAS can improve communication rates in simultaneous wireless information and power transfer (SWIPT) systems.

Integrated sensing and communication (ISAC) is an emerging technology that unifies the traditionally separate functions of sensing and communication within a single system [22], [23]. A key challenge in ISAC lies in balancing communication and sensing performance while sharing the same time-frequency resource unit and hardware resources. The FAS, with its ability to dynamically alter propagation channels, introduces a new DoF that can enhance ISAC performance [6], [24]. In [25], deep reinforcement learning (DRL) is employed to optimize the downlink sum rate under sensing constraints in a FAS-assisted multiuser multiple-input multiple-output (MIMO) system. Furthermore, [26] derives closed-form expressions for the outage probability and ergodic sensing rate (ESR) in a two-user NOMA-ISAC system, where both users are equipped with two-dimensional (2D) FASs.

In this paper, we investigate an ISAC system comprising a downlink user, an uplink user, and a sensing target. The primary motivation is to assess whether the FAS can provide the base station (BS) with sufficient self-interference (SI) cancellation capability to support full-duplex communication while

simultaneously performing ISAC operations. Our goal is to maximize the system's communication rate while guaranteeing satisfactory sensing performance. Given that SI in full-duplex systems can limit ISAC effectiveness, we jointly optimize the transmit and receive antenna positions, beamforming vectors, and the uplink user's transmit power to tackle this issue.

# II. SYSTEM MODEL AND PROBLEM FORMULATION A. Signal Model

Here, we study a full-duplex ISAC system assisted by FAS, in which a BS simultaneously serves a downlink user, an uplink user, and performs single target sensing. The transmitter and the receiver of the BS are an M-antenna planar FAS and an N-antenna planar FAS, respectively. The size of each FAS is given as  $S = [0, W] \times [0, W]$ . The positions of the m-th transmit antenna and the n-th receive antenna are  $\boldsymbol{v}_m = [x_m^{\rm t}, y_m^{\rm t}]^T$  and  $\boldsymbol{u}_n = [x_n^{\rm r}, y_n^{\rm r}]^T$ , respectively. The users are equipped with fixed-position antennas (FPAs).

The signal received by the downlink user is written as

$$y_{d} = \boldsymbol{h}_{d}(\boldsymbol{V})\boldsymbol{w}_{t}s_{d} + n_{d}, \tag{1}$$

where  $m{h}_{ ext{d}}(m{V}) \in \mathbb{C}^{1 imes M}$  denotes the channel from the BS to the downlink user,  $V = [v_1, \dots, v_M] \in \mathbb{R}^{2 \times M}$ ,  $w_t \in \mathbb{C}^{M \times 1}$  is the precoding vector at the BS,  $s_d \sim \mathcal{CN}(0,1)$  is the transmitted symbol, and  $n_{\rm d} \sim \mathcal{CN}(0, \sigma_{\rm d}^2)$  is the additive noise.

The received signal of the BS is given by

$$y_{\rm r} = h_{\rm u}(U)\sqrt{p_{\rm u}}s_{\rm u} + (H_{\rm s}(V,U) + H_{\rm SI}(V,U))w_{\rm t}s_{\rm d} + n_{\rm r},$$
(2)

where  $p_{\rm u}$  and  $s_{\rm u} \sim \mathcal{CN}(0,1)$  are the transmit power and the symbol of the uplink user, respectively,  $h_{\rm u}(U)\in\mathbb{C}^{N\times 1}$  is the uplink channel,  $U=[u_1,\ldots,u_N]\in\mathbb{R}^{2\times N},\ H_{\rm s}\in\mathbb{C}^{N\times M}$  and  $H_{\rm SI}\in\mathbb{C}^{N\times M}$  are the sensing and SI channels, respectively. tively, and  $n_r \sim \mathcal{CN}(\mathbf{0}, \sigma_r^2 \mathbf{I})$  is the additive noise.

#### B. Channel Model

Denote the angle-of-departures (AoDs) and angle-of-arrivals (AoAs) of the channel by  $(\phi_l^t, \theta_l^t)$  and  $(\phi_l^r, \theta_l^r)$ , respectively. The receive and transmit steering vectors of the channel are

$$\mathbf{r}_{l}(\mathbf{U}) = \left[ e^{-j\frac{2\pi}{\lambda}\rho_{l}^{t}(\mathbf{u}_{1})}, \dots, e^{-j\frac{2\pi}{\lambda}\rho_{l,l}(\mathbf{u}_{N})} \right]^{T} \in \mathbb{C}^{N \times 1},$$

$$\mathbf{t}_{l}(\mathbf{V}) = \left[ e^{-j\frac{2\pi}{\lambda}\rho_{l}^{t}(\mathbf{v}_{1})}, \dots, e^{-j\frac{2\pi}{\lambda}\rho_{l}^{t}(\mathbf{v}_{M})} \right]^{T} \in \mathbb{C}^{M \times 1}, \quad (3)$$

where  $\rho_l^{\rm r}(\boldsymbol{u}_n) \triangleq x_n^{\rm r} \delta_l^{\rm r} + y_n^{\rm r} \xi_l^{\rm r}$  with  $\delta_l^{\rm r} = \sin \theta_l^{\rm r} \cos \phi_l^{\rm r}$  and  $\xi_l^{\rm r} =$  $\cos \theta_l^{\rm r}$ , and  $\rho_l^{\rm t}(\boldsymbol{v}_m) \stackrel{\triangle}{=} x_m^{\rm t} \delta_l^{\rm t} + y_m^{\rm t} \xi_l^{\rm t}$  with  $\delta_l^{\rm t} = \sin \theta_l^{\rm t} \cos \phi_l^{\rm t}$  and  $\xi_l^{\rm t} = \cos \theta_l^{\rm t}$ . Let L denote the number of propagation paths of the channel. Then, the general channel can be written as

$$H(V, U) = R(U)\Gamma T^{H}(V) \in \mathbb{C}^{N \times M},$$
 (4)

where  $\Gamma = \operatorname{diag}\{\gamma^1, \dots, \gamma^L\} \in \mathbb{C}^{L \times L}$  denotes the channel coefficient matrix,  $R(U) = [r_1(U), \dots, r_L(U)] \in \mathbb{C}^{N \times L}$ and  $T(V) = [t_1(V), \dots, t_L(V)] \in \mathbb{C}^{M \times L}$ .

Since both the transmitter and the receiver of the SI channel are FASs, the SI channel follows the definition in (4), which is written as

$$H_{SI}(V, U) = R_{SI}(U)\Gamma_{SI}T_{SI}^{H}(V) \in \mathbb{C}^{N \times M}.$$
 (5)

Considering FPAs at the users, the downlink and the uplink channels can be written as

$$h_{d}(\mathbf{V}) = \mathbf{1}^{H} \mathbf{\Gamma}_{d} \mathbf{T}_{d}^{H}(\mathbf{V}) \in \mathbb{C}^{1 \times M},$$
 (6)

$$\boldsymbol{h}_{\mathrm{u}}(\boldsymbol{U}) = \boldsymbol{R}_{\mathrm{u}}(\boldsymbol{U})\boldsymbol{\Gamma}_{\mathrm{u}}\boldsymbol{1} \in \mathbb{C}^{N \times 1},$$
 (7)

where 1 is an all-ones column vector.

For the sensing task, we consider a mono-static radar where the AoA and AoD of the sensing channel are equal. Since the number of sensing paths is one, the sensing channel can thus be written as

$$H_{s}(V, U) = \alpha_{s} R_{s}(U) T_{s}^{H}(V) \in \mathbb{C}^{N \times M},$$
 (8)

where  $\alpha_s$  is the reflection coefficient including the path loss and the radar cross section (RCS).

#### C. Optimization Problem

In this paper, our target is to maximize the communication sum rate under sensing constraint by optimizing the antenna positions, beamforming design, and the uplink transmit power. Denote the linear beamformer adopted by the BS for detecting  $s_{\mathbf{u}}$  by  $\mathbf{w}_{\mathbf{r}} \in \mathbb{C}^{N \times 1}$ . The problem can be written as

$$\max_{\boldsymbol{\Phi}} f_0(\boldsymbol{\Phi}) = \log (1 + \eta_{d}(\boldsymbol{V}, \boldsymbol{w}_{t})) + \log (1 + \eta_{u}(\boldsymbol{\Phi}))$$
(9a)

s.t. 
$$\eta_s(\boldsymbol{\Phi}) \ge \eta$$
, (9b)

$$\|\boldsymbol{w}_{\mathsf{t}}\|^2 \le P_{\mathsf{t}},\tag{9c}$$

$$0 \le p_{\mathbf{u}} \le P_{\mathbf{u}},\tag{9d}$$

$$\boldsymbol{v}_{m}, \boldsymbol{v}_{m'} \in \mathcal{S}, \boldsymbol{v}_{m} \neq \boldsymbol{v}_{m'}, \ \forall m, m' \in \mathcal{M}, m \neq m',$$
(9e)

$$u_n, u_{n'} \in \mathcal{S}, u_n \neq u_{n'}, \ \forall n, n' \in \mathcal{N}, n \neq n',$$
 (9f)

where 
$$\eta_{\rm d}(m{V}) = \frac{|m{h}_{\rm d}(m{V})m{w}_{\rm t}|^2}{\sigma_{\rm d}^2}$$
 is the downlink SINR,  $\eta_{\rm u}(m{V}, m{U}) = \frac{p_{\rm u} \big| m{w}_{\rm r}^H m{h}_{\rm u}(m{U}) \big|^2}{|m{w}_{\rm r}^H m{H}(m{V}, m{U}) m{w}_{\rm t}|^2 + \sigma_{\rm r}^2 ||m{w}_{\rm r}^H||^2}$  is the uplink SINR,  $\eta_{\rm s}(m{V}, m{U}) = \frac{\big| m{w}_{\rm r}^H m{H}_{\rm s}(m{V}, m{U}) m{w}_{\rm t} \big|^2}{\| m{w}_{\rm r}^H m{H}_{\rm s}(m{V}, m{U}) m{w}_{\rm t} \big|^2}$  is the sensing SINR

 $\begin{array}{l} \frac{\|\boldsymbol{w}_{\mathrm{f}}\|\boldsymbol{A}_{\mathrm{S}}(\boldsymbol{V},\boldsymbol{V})\boldsymbol{\omega}_{\mathrm{I}}\|}{p_{\mathrm{u}}|\boldsymbol{w}_{\mathrm{f}}^{H}\boldsymbol{h}_{\mathrm{u}}(\boldsymbol{U})|^{2}+|\boldsymbol{w}_{\mathrm{f}}^{H}\boldsymbol{H}_{\mathrm{SI}}(\boldsymbol{V},\boldsymbol{U})\boldsymbol{w}_{\mathrm{t}}|^{2}+\sigma_{\mathrm{f}}^{2}||\boldsymbol{w}_{\mathrm{f}}^{H}||^{2}}{\boldsymbol{H}(\boldsymbol{V},\boldsymbol{U})=\boldsymbol{H}_{\mathrm{S}}(\boldsymbol{V},\boldsymbol{U})+\boldsymbol{H}_{\mathrm{SI}}(\boldsymbol{V},\boldsymbol{U}),\;\eta\;\mathrm{is\;the\;sensing\;SINR} \end{array}$ threshold,  $P_{t}$  and  $P_{u}$  are the maximum transmit power of the BS and the uplink user,  $\Phi = \{V, U, w_t, w_r, p_u\}$  contains all the optimizing variables, and  $\mathcal{M} = \{1, \dots, M\}$  and  $\mathcal{N} = \{1, \dots, N\}$  denote the index sets of the transmit and receive antennas, respectively.

#### III. PROBLEM SOLUTION

Since (9) is non-convex, we first remove the optimization variables from the log operation in (9a) by introducing auxiliary variables  $\Delta = \{\Delta_d, \Delta_u\}$  and transform  $f_0(\Phi)$  to

$$f_1(\boldsymbol{\Phi}, \boldsymbol{\Delta}) = \log(1 + \Delta_d) - \Delta_d + \frac{(1 + \Delta_d)|\boldsymbol{h}_d(\boldsymbol{V})\boldsymbol{w}_t|^2}{|\boldsymbol{h}_d(\boldsymbol{V})\boldsymbol{w}_t|^2 + \sigma_d^2} + \log(1 + \Delta_u)$$

$$-\Delta_{\mathbf{u}} + \frac{(1 + \Delta_{\mathbf{u}})p_{\mathbf{u}} \left| \boldsymbol{w}_{\mathbf{r}}^{H} \boldsymbol{h}_{\mathbf{u}}(\boldsymbol{U}) \right|^{2}}{p_{\mathbf{u}} \left| \boldsymbol{w}_{\mathbf{r}}^{H} \boldsymbol{h}_{\mathbf{u}}(\boldsymbol{U}) \right|^{2} + \left| \boldsymbol{w}_{\mathbf{r}}^{H} \boldsymbol{H}(\boldsymbol{V}, \boldsymbol{U}) \boldsymbol{w}_{\mathbf{t}} \right|^{2} + \sigma_{\mathbf{r}}^{2} \|\boldsymbol{w}_{\mathbf{r}}^{H}\|^{2}}.$$
 (10)

For fixed  $\Phi$ , by setting  $\frac{\partial f_1}{\partial \Delta_0}$  and  $\frac{\partial f_1}{\partial \Delta_0}$  to zero, the optimal  $f_1$ can be obtained at

$$\Delta_{d}^{*} = \frac{\left|\boldsymbol{h}_{d}(\boldsymbol{V})\boldsymbol{w}_{t}\right|^{2}}{\sigma_{d}^{2}}, \Delta_{u}^{*} = \frac{p_{u}\left|\boldsymbol{w}_{r}^{H}\boldsymbol{h}_{u}(\boldsymbol{U})\right|^{2}}{\left|\boldsymbol{w}_{r}^{H}\boldsymbol{H}(\boldsymbol{V},\boldsymbol{U})\boldsymbol{w}_{t}\right|^{2} + \sigma_{r}^{2}\|\boldsymbol{w}_{r}^{H}\|^{2}}.$$
(11)

which satisfies  $f_1(\Phi, \Delta^*) = f_0(\Phi)$ . Problem (9) can thus be equivalently written as

$$egin{array}{ll} \max & f_1(oldsymbol{arPhi},oldsymbol{\Delta}) \\ ext{s.t.} & f_s(oldsymbol{arPhi}) \geq 0, \\ & (9e), (9d), (9e), (9f), \end{array}$$

where  $f_{\rm s}(\boldsymbol{\Phi}) = \left|\boldsymbol{w}_{\rm r}^H\boldsymbol{H}_{\rm s}(\boldsymbol{V},\boldsymbol{U})\boldsymbol{w}_{\rm t}\right|^2 - \eta \left(p_{\rm u}\left|\boldsymbol{w}_{\rm r}^H\boldsymbol{h}_{\rm u}(\boldsymbol{U})\right|^2 + \left|\boldsymbol{w}_{\rm r}^H\boldsymbol{H}_{\rm SI}(\boldsymbol{V},\boldsymbol{U})\boldsymbol{w}_{\rm t}\right|^2 + \sigma_{\rm r}^2\|\boldsymbol{w}_{\rm r}^H\|^2\right)$ . Also,  $f_1(\boldsymbol{\Phi},\boldsymbol{\Delta})$  can be further simplified by introducing auxiliary variables  $\boldsymbol{\omega} = \{\omega_{\rm d},\omega_{\rm u}\}$  as

$$f_{2}(\boldsymbol{\Phi}, \boldsymbol{\Delta}, \boldsymbol{\omega}) = \log(1 + \Delta_{d}) - \Delta_{d}$$

$$+ (1 + \Delta_{d}) \left[ 2\operatorname{Re} \{ \omega_{d}^{H} \boldsymbol{h}_{d}(\boldsymbol{V}) \boldsymbol{w}_{t} \} - |\omega_{d}|^{2} \left( |\boldsymbol{h}_{d}(\boldsymbol{V}) \boldsymbol{w}_{t}|^{2} + \sigma_{d}^{2} \right) \right]$$

$$+ \log(1 + \Delta_{u}) - \Delta_{u} + p_{u}(1 + \Delta_{u}) \left[ 2\operatorname{Re} \{ \omega_{u}^{H} \boldsymbol{w}_{r}^{H} \boldsymbol{h}_{u}(\boldsymbol{U}) \} \right]$$

$$- |\omega_{u}|^{2} \left( p_{u} |\boldsymbol{w}_{r}^{H} \boldsymbol{h}_{u}(\boldsymbol{U})|^{2} + |\boldsymbol{w}_{r}^{H} \boldsymbol{H}(\boldsymbol{V}, \boldsymbol{U}) \boldsymbol{w}_{t}|^{2} + \sigma_{r}^{2} ||\boldsymbol{w}_{r}^{H}||^{2} \right) , \tag{13}$$

which has the optimal values at

$$\omega_{d}^{*} = \frac{\boldsymbol{h}_{d}(\boldsymbol{V})\boldsymbol{w}_{t}}{|\boldsymbol{h}_{d}(\boldsymbol{V})\boldsymbol{w}_{t}|^{2} + \sigma_{d}^{2}},$$

$$\omega_{u}^{*} = \frac{\boldsymbol{w}_{r}^{H}\boldsymbol{h}_{u}(\boldsymbol{U})}{p_{u}|\boldsymbol{w}_{r}^{H}\boldsymbol{h}_{u}(\boldsymbol{U})|^{2} + |\boldsymbol{w}_{r}^{H}\boldsymbol{H}(\boldsymbol{V}, \boldsymbol{U})\boldsymbol{w}_{t}|^{2} + \sigma_{r}^{2}||\boldsymbol{w}_{r}^{H}||^{2}}.$$
(14)

Since  $f_2(\Phi, \Delta, \omega^*) = f_1(\Phi, \Delta)$ , problem (12) can be reformulated as

$$\begin{aligned} \max_{\boldsymbol{\Phi},\boldsymbol{\Delta},\boldsymbol{\omega}} & f_2(\boldsymbol{\Phi},\boldsymbol{\Delta},\boldsymbol{\omega}) \\ \text{s.t.} & f_s(\boldsymbol{V},\boldsymbol{U}) \geq 0, \\ & (9c), (9d), (9e), (9f). \end{aligned} \tag{15}$$

Since problem (15) is still non-convex, we iteratively update each variable in the following.

A. Updating Transmit Antenna Positions

With fixed  $\{U, w_t, w_r, p_u, \Delta, \omega\}$ , (15) becomes

$$\max_{\boldsymbol{V}} \alpha_{d} \left( 2\operatorname{Re}\{\omega_{d}^{H}\boldsymbol{1}^{H}\boldsymbol{\Gamma}_{d}\boldsymbol{T}_{d}^{H}(\boldsymbol{V})\boldsymbol{w}_{t}\} - |\omega_{d}|^{2} |\boldsymbol{1}^{H}\boldsymbol{\Gamma}_{d}\boldsymbol{T}_{d}^{H}(\boldsymbol{V})\boldsymbol{w}_{t}|^{2} \right) \\ -\alpha_{u} \left( \left| \alpha_{s}\boldsymbol{w}_{r}^{H}\boldsymbol{a}_{r}\boldsymbol{T}_{s}^{H}(\boldsymbol{V})\boldsymbol{w}_{t} \right|^{2} + \left| \boldsymbol{w}_{r}^{H}\boldsymbol{R}_{SI}\boldsymbol{\Gamma}_{SI}\boldsymbol{T}_{SI}^{H}(\boldsymbol{V})\boldsymbol{w}_{t} \right|^{2} \\ + 2\operatorname{Re}\left\{ \left( \alpha_{s}\boldsymbol{w}_{r}^{H}\boldsymbol{a}_{r}\boldsymbol{T}_{s}^{H}(\boldsymbol{V})\boldsymbol{w}_{t} \right) \left( \boldsymbol{w}_{r}^{H}\boldsymbol{R}_{SI}\boldsymbol{\Gamma}_{SI}\boldsymbol{T}_{SI}^{H}(\boldsymbol{V})\boldsymbol{w}_{t} \right)^{H} \right\} \right) \\ \text{s.t.} \quad \eta \left| \boldsymbol{w}_{r}^{H}\boldsymbol{R}_{SI}\boldsymbol{\Gamma}_{SI}\boldsymbol{T}_{SI}^{H}(\boldsymbol{V})\boldsymbol{w}_{t} \right|^{2} - \left| \alpha_{s}\boldsymbol{w}_{r}^{H}\boldsymbol{a}_{r}\boldsymbol{T}_{s}^{H}(\boldsymbol{V})\boldsymbol{w}_{t} \right|^{2} \leq -\beta_{1}, \\ (9e), \tag{16}$$

where  $\alpha_d = 1 + \Delta_d$ ,  $\alpha_u = p_u(1 + \Delta_u)|\omega_u|^2$ , and  $\beta_1 = \eta \left(p_u \left| \boldsymbol{w}_r^H \boldsymbol{h}_u \right|^2 + \sigma_r^2 ||\boldsymbol{w}_r^H||^2\right)$ . Since the problem is still nonconvex and intractable, we solve it using successive convex approximation (SCA). For convenience, denote  $\boldsymbol{v} = \text{vector}\{\boldsymbol{V}\} = [x_1^t, \dots, x_M^t, y_1^t, \dots, y_M^t]^T = [v_1, \dots, v_{2M}]^T$ .

**Theorem 1.** For arbitrary vectors  $\mathbf{a} = [a_1, \dots, a_L]^T$  and  $\mathbf{b} = [b_1, \dots, b_M]^T$ ,  $\mathbf{v}^T \hat{\mathbf{\Lambda}} \mathbf{v} + \hat{\mathbf{c}} \mathbf{v} + \hat{d}$  and  $-\mathbf{v}^T \hat{\mathbf{\Lambda}} \mathbf{v} + \bar{\mathbf{c}} \mathbf{v} + \bar{d}$  are concave and convex quadratic surrogate functions for

 $|\boldsymbol{a}^T \boldsymbol{T}_{\chi_1}^H(\boldsymbol{V}) \boldsymbol{b}|^2$  respectively, where  $\chi_1 \in \{d, SI, s\}$ , and  $\hat{\boldsymbol{\Lambda}}$  is a negative semi-definite (NSD) matrix.

*Proof:*  $|\boldsymbol{a}^T \boldsymbol{T}_{\chi_1}^H(\boldsymbol{V}) \boldsymbol{b}|^2$  can first be transformed into  $\cos$  functions. Its upper and lower bounds can then be obtained using the second order Taylor expansion, written in the matrix form as  $\boldsymbol{v}^T \hat{\boldsymbol{\Lambda}} \boldsymbol{v} + \hat{\boldsymbol{c}} \boldsymbol{v} + \hat{\boldsymbol{d}}$  and  $-\boldsymbol{v}^T \hat{\boldsymbol{\Lambda}} \boldsymbol{v} + \bar{\boldsymbol{c}} \boldsymbol{v} + \bar{\boldsymbol{d}}$ . The details are omitted in this paper due to space limitations.

**Lemma 1.** A concave quadratic surrogate function for  $Re\{a^TT_{\chi_1}^H(V)b\}$  is given by  $v^T\tilde{\Lambda}v + \tilde{c}v + \tilde{d}$ , where  $\chi_1 \in \{d, SI, s\}$ , and  $\tilde{\Lambda}$  is an NSD matrix.

*Proof:* Similar to the proof of Theorem 1.

**Lemma 2.** For any vectors  $\mathbf{a} = [a_1, \dots, a_L]^T$ ,  $\mathbf{b} = [b_1, \dots, b_M]^T$ , and  $\check{\mathbf{a}} = [\check{a}_1, \dots, \check{a}_{\check{L}}]^T$ , a convex quadratic surrogate function for  $\operatorname{Re}\{(\mathbf{a}^T\mathbf{T}^H_\chi(\mathbf{V})\mathbf{b})(\check{\mathbf{a}}^T\mathbf{T}^H_\chi(\mathbf{V})\mathbf{b})^H\}$  can be expressed as  $\mathbf{v}^T\check{\mathbf{A}}\mathbf{v} + \check{\mathbf{c}}\mathbf{v} + \check{\mathbf{d}}$ , where  $\chi, \check{\chi} \in \{d, SI, s\}, \chi \neq \check{\chi}$ ,  $\check{\mathbf{A}}$  is a positive semi-definite (PSD) matrix.

*Proof:* Similar to the proof of Theorem 1.

According to Theorem 1, a concave quadratic surrogate function of  $\left|\alpha_s \boldsymbol{w}_r^H \boldsymbol{a}_r \boldsymbol{T}_s^H(\boldsymbol{V}) \boldsymbol{w}_t \right|^2$  can be written as  $\boldsymbol{v}^T \hat{\boldsymbol{\Lambda}}_s \boldsymbol{v} + \hat{\boldsymbol{c}}_s \boldsymbol{v} + \hat{\boldsymbol{d}}_s$ . In addition, we can obtain the convex quadratic surrogate functions of  $\left| \mathbf{1}^H \boldsymbol{\Gamma}_d \mathbf{T}_d^H(\boldsymbol{V}) \boldsymbol{w}_t \right|^2$ ,  $\left| \alpha_s \boldsymbol{w}_r^H \boldsymbol{a}_r \mathbf{T}_s^H(\boldsymbol{V}) \boldsymbol{w}_t \right|^2$ , and  $\left| \boldsymbol{w}_r^H \boldsymbol{R}_{\text{SI}} \boldsymbol{\Gamma}_{\text{SI}} \boldsymbol{T}_{\text{SI}}^H(\boldsymbol{V}) \boldsymbol{w}_t \right|^2$  as  $-\boldsymbol{v}^T \hat{\boldsymbol{\Lambda}}_d \boldsymbol{v} + \bar{\boldsymbol{c}}_d \boldsymbol{v} + \bar{\boldsymbol{d}}_d$ ,  $-\boldsymbol{v}^T \hat{\boldsymbol{\Lambda}}_s \boldsymbol{v} + \bar{\boldsymbol{c}}_s \boldsymbol{v} + \bar{\boldsymbol{d}}_s$ , and  $-\boldsymbol{v}^T \hat{\boldsymbol{\Lambda}}_{\text{SI}} \boldsymbol{v} + \bar{\boldsymbol{c}}_{\text{SI}} \boldsymbol{v} + \bar{\boldsymbol{d}}_{\text{SI}}$ . Based on Lemma 1, a concave quadratic surrogate function of  $\operatorname{Re}\{\omega_d^H \mathbf{1}^H \boldsymbol{\Gamma}_d \mathbf{T}_d^H(\boldsymbol{V}) \boldsymbol{w}_t\}$  can be obtained as  $\boldsymbol{v}^T \tilde{\boldsymbol{\Lambda}}_d \boldsymbol{v} + \tilde{\boldsymbol{c}}_d \boldsymbol{v} + \tilde{\boldsymbol{d}}_d$ . Using Lemma 2, a convex quadratic surrogate function for  $\operatorname{Re}\{(\alpha_s \boldsymbol{w}_r^H \boldsymbol{a}_r \boldsymbol{T}_s^H(\boldsymbol{V}) \boldsymbol{w}_t) \big| (\boldsymbol{w}_r^H \boldsymbol{R}_{\text{SI}} \boldsymbol{\Gamma}_{\text{SI}} \boldsymbol{T}_{\text{SI}}^H(\boldsymbol{V}) \boldsymbol{w}_t)^H\}$  can be written as  $\boldsymbol{v}^T \tilde{\boldsymbol{\Lambda}}_{\text{SSI}} \boldsymbol{v} + \check{\boldsymbol{c}}_{\text{SSI}} \boldsymbol{v} + \check{\boldsymbol{d}}_{\text{SI}}.$ 

Problem (16) can then be transformed to

$$\max_{\boldsymbol{v}} \quad \boldsymbol{v}^T \boldsymbol{\Lambda}_1 \boldsymbol{v} + \boldsymbol{c}_1 \boldsymbol{v} + d_1, \tag{17a}$$

s.t. 
$$\mathbf{v}^T \mathbf{\Lambda}_2 \mathbf{v} + \mathbf{c}_2 \mathbf{v} + d_2 \le -\beta_1,$$
 (17b)

$$0 \le v_m \le W, m = 1, \dots, 2M,$$
 (17c)

$$[v_m, v_{m+M}] \neq [v_{m'}, v_{m'+M}], \ \forall m, m' \in \mathcal{M}, m \neq m',$$
(17d)

where  $\boldsymbol{\Lambda}_1 = \alpha_{\rm d}(2\tilde{\boldsymbol{\Lambda}}_{\rm d} + |\omega_{\rm d}|^2\hat{\boldsymbol{\Lambda}}_{\rm d}) + \alpha_{\rm u}(\hat{\boldsymbol{\Lambda}}_{\rm s} + \hat{\boldsymbol{\Lambda}}_{\rm SI} - 2\check{\boldsymbol{\Lambda}}_{\rm sSI}),$   $\boldsymbol{c}_1 = \alpha_{\rm d}(2\tilde{\boldsymbol{c}}_{\rm d} - |\omega_{\rm d}|^2\bar{\boldsymbol{c}}_{\rm d}) - \alpha_{\rm u}(\bar{\boldsymbol{c}}_{\rm s} + \bar{\boldsymbol{c}}_{\rm SI} + 2\check{\boldsymbol{c}}_{\rm sSI}), \ d_1 = \alpha_{\rm d}(2\tilde{d}_{\rm d} - |\omega_{\rm d}|^2\bar{d}_{\rm d}) - \alpha_{\rm u}(\bar{d}_{\rm s} + \bar{d}_{\rm SI} + 2\check{d}_{\rm sSI}), \ \boldsymbol{\Lambda}_2 = -\eta\hat{\boldsymbol{\Lambda}}_{\rm SI} - \hat{\boldsymbol{\Lambda}}_{\rm s}, \ \boldsymbol{c}_2 = \eta\bar{\boldsymbol{c}}_{\rm SI} - \hat{\boldsymbol{c}}_{\rm s}, \ \text{and} \ d_2 = \eta\bar{d}_{\rm SI} - \hat{\boldsymbol{d}}_{\rm s}.$ 

By omitting (17d), (17) becomes convex and can be efficiently solved using CVX. The quadratic surrogate functions in Theorem 1, Lemma 1, and Lemma 2 are constructed using Taylor series expansions around the given antenna positions  $V_0$ . Based on this, we employ the SCA method to address (16). Specifically, the SCA algorithm is initialized with a feasible v that satisfies (17d), and at each iteration, v is updated only if the updated solution satisfies (17d).

## B. Updating Receive Antenna Positions

The positions of the receive FAS can be optimized using the method in the above section of optimizing transmit antenna positions. The details are omitted here due to the space limit.

#### C. Updating Transmit and Receive Beamforming Vectors

With fixed  $\{V, U, w_r, p_u, \Delta, \omega\}$ , (15) becomes a convex quadratic problem except for a constraint in the difference of convex (DC) form. Using Taylor series expansion, a convex lower-bound of the DC constraint can be obtained. The transmit beamforming vector  $w_t$  can then be iteratively optimized using CVX. Considering fixed  $\{V, U, w_t, p_u, \Delta, \omega\}$ , the receive beamforming vector  $w_t$  can be optimized similar to  $w_t$ .

## D. Updating Uplink Transmit Power

With fixed  $\{V, U, w_t, w_r, \Delta, \omega\}$ , the optimal value of  $p_u$  can be obtained at

$$p_{\mathbf{u}}^* = \min\left\{\max\left\{\frac{\alpha_2}{2\alpha_1}, 0\right\}, \min\{\alpha_3, P_{\mathbf{u}}\}\right\}, \quad (18)$$

where  $\alpha_1 = |\omega_{\mathbf{u}}|^2 |\boldsymbol{w}_{\mathbf{r}}^H \boldsymbol{h}_{\mathbf{u}}|^2$ ,  $\alpha_2 = 2 \operatorname{Re} \{ \omega_{\mathbf{u}}^H \boldsymbol{w}_{\mathbf{r}}^H \boldsymbol{h}_{\mathbf{u}} \} - |\omega_{\mathbf{u}}|^2 ( |\boldsymbol{w}_{\mathbf{r}}^H \boldsymbol{H} \boldsymbol{w}_{\mathbf{t}}|^2 + \sigma_{\mathbf{r}}^2 ||\boldsymbol{w}_{\mathbf{r}}^H||^2 )$ , and  $\alpha_3 = [|\boldsymbol{w}_{\mathbf{r}}^H \boldsymbol{H}_{\mathbf{s}} \boldsymbol{w}_{\mathbf{t}}|^2 - \eta ( |\boldsymbol{w}_{\mathbf{r}}^H \boldsymbol{H}_{\mathbf{SI}} \boldsymbol{w}_{\mathbf{t}}|^2 + \sigma_{\mathbf{r}}^2 ||\boldsymbol{w}_{\mathbf{r}}^H ||^2 )] / (\eta ||\boldsymbol{w}_{\mathbf{r}}^H \boldsymbol{h}_{\mathbf{u}}|^2 )$ .

# E. Updating Auxiliary Variables

The optimal values of  $\Delta$  and  $\omega$  are derived from equations (11) and (14), respectively.

#### IV. SIMULATION RESULTS

In this section, we evaluate the performance of the proposed algorithms using Monte-Carlo simulations. The transmit frequency is 30 GHz. The azimuth and elevation AoAs and AoDs follow uniform distribution over  $[0,\pi]$ . For convenience, we assume that the number of propagation paths is equal, i.e.,  $L_{\rm d}=L_{\rm u}=L_{\rm SI}=L$ . Considering unit noise power, the maximum transmit signal-to-noise ratios (SNRs) of the BS and the uplink user are  ${\rm SNR_t}=10\,{\rm lg}\,{\rm P_t}$  dB and  ${\rm SNR_u}=10\,{\rm lg}\,{\rm P_u}$  dB. Unless otherwise specified, we set  $W=5\lambda$ , M=N=L=2,  $\alpha_s=10$ ,  $\eta=1$ ,  ${\rm SNR_t}=10\,{\rm dB}$ , and  ${\rm SNR_u}=7\,{\rm dB}$  in the simulations. We compare the proposed algorithm with the following benchmarks:

- **FPA:** To evaluate the performance, the communication rate achieved by the traditional FPA scheme, with the antenna spacing of  $\lambda/2$ , is given as a benchmark.
- Transmit FAS (FAS-Tx): The BS transmits signals using FAS while receiving signals using FPA. The positions of the transmit FAS V are optimized while the positions of FPA are spaced by  $\lambda/2$ .
- Receive FAS (FAS-Rx): The BS transmits signals using FPA while receiving signals using FAS. The positions of the receive FAS U are optimized while the positions of FPA are spaced by λ/2.

To distinguish from the benchmarks, we use "FAS-Tx+Rx" to indicate the considered case where both the transmitter and the receiver of the BS are equipped with FAS.

Fig. 1 depicts the communication rate as a function of the number of transmit antennas at the base station. The performance gap between the FAS and the FPA increases with larger M. Specifically, when M=10, optimizing the positions of the transmit FAS antennas results in a  $3.4~\rm bps/Hz$  gain over

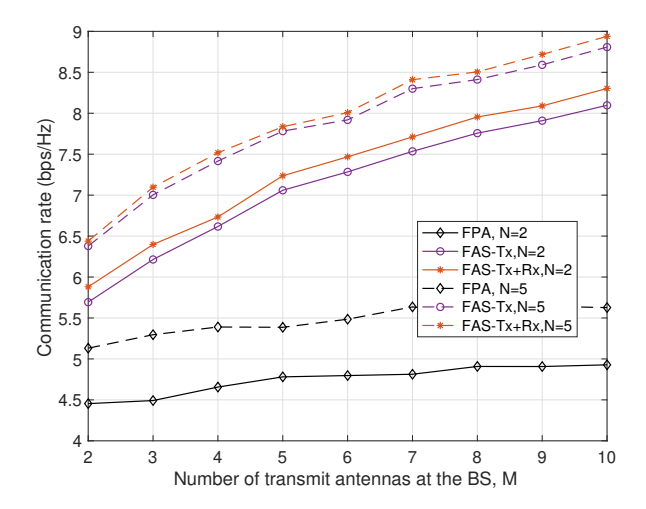


Fig. 1. Communication rate versus the number of transmit BS antennas, M.

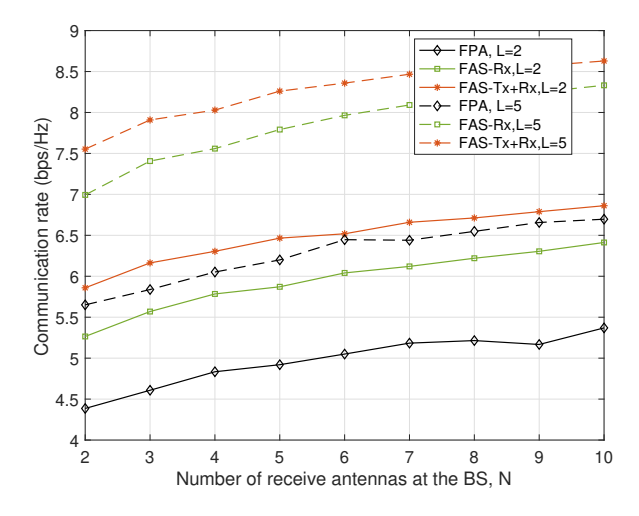


Fig. 2. Communication rate versus the number of receive BS antennas, N.

the FPA, corresponding to approximately a 68% improvement. While optimizing the transmit FAS alone substantially boosts the communication rate, jointly optimizing both transmit and receive FAS positions yields even greater performance gains.

Fig. 2 studies the impact of the number of receive antennas at the BS on the communication rate. Optimizing the positions of the receive antennas increases the communication rate by  $1.5~{\rm bps/Hz}$  and  $2~{\rm bps/Hz}$  compared to the FPA scheme for  $L=2~{\rm and}~L=5$ , respectively. Moreover, jointly optimizing both transmit and receive FAS positions provides an additional gain of  $0.5~{\rm bps/Hz}$  beyond optimizing the receive FAS alone.

Fig. 3 illustrates the relationship between the communication rate and the number of propagation paths. The results indicate that optimizing the transmit FAS outperforms optimizing the receive FAS alone. This advantage arises because both uplink and downlink rates depend on the BS's transmitter, whereas the receiver only affects the uplink rate. Furthermore, jointly optimizing both transmit and receive FAS

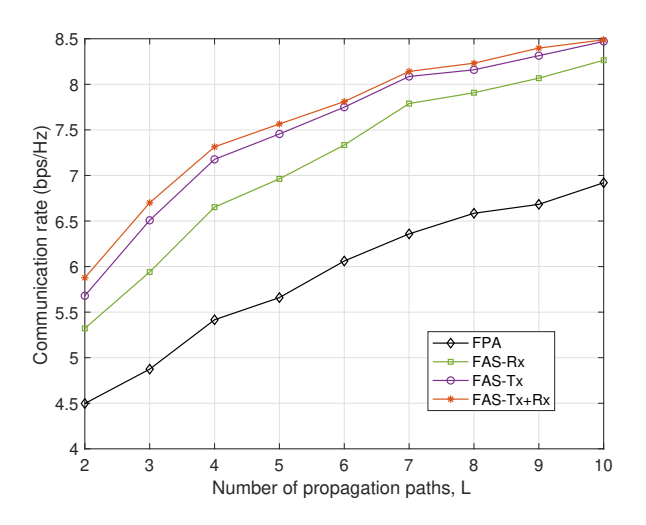


Fig. 3. Communication rate versus the number of propagation paths, L.

positions achieves the highest communication rate, providing a 1.5 bps/Hz gain over the FPA scheme.

#### V. CONCLUSION

In this paper, we addressed the problem of maximizing the communication rate while satisfying sensing performance constraints. We first employed the fractional programming (FP) framework to reformulate the problem, enabling iterative optimization of each variable. Next, we developed an SCA-based approach to optimize the antenna positions by converting the relevant subproblems into convex forms. Simulation results demonstrate that, with the proposed algorithm, FAS significantly outperform FPA in achieving higher communication rates within full-duplex ISAC systems.

#### REFERENCES

- Y. Zeng et al., "A tutorial on environment-aware communications via channel knowledge map for 6G," IEEE Commun. Surveys Tuts., vol. 26, no. 3, pp. 1478–1519, 3rd Quart. 2024.
- [2] M. Giordani, M. Polese, M. Mezzavilla, S. Rangan, and M. Zorzi, "Toward 6G networks: Use cases and technologies," *IEEE Commun. Mag.*, vol. 58, no. 3, pp. 55–61, Mar. 2020.
- [3] X. You et al., "Toward 6G TKμ extreme connectivity: Architecture, key technologies and experiments," *IEEE Wireless Commun.*, vol. 30, no. 3, pp. 86–95, Jun. 2023.
- [4] F. Tariq et al., "A speculative study on 6G," IEEE Wireless Commun., vol. 27, no. 4, pp. 118–125, Aug. 2020.
- [5] K.-K. Wong, A. Shojaeifard, K.-F. Tong, and Y. Zhang, "Fluid antenna systems," *IEEE Trans. Wireless Commun.*, vol. 20, no. 3, pp. 1950–1962, Mar. 2021.
- [6] W. K. New et al., "A tutorial on fluid antenna system for 6G networks: Encompassing communication theory, optimization methods and hard-ware designs," *IEEE Commun. Surv. Tuts.*, early access, doi:10.1109/COMST.2024.3498855, 2024.
- [7] K.-K. Wong, C.-B. Chae, and K.-F. Tong, "Compact ultra massive antenna array: A simple open-loop massive connectivity scheme," *IEEE Trans. Wireless Commun.*, vol. 23, no. 6, pp. 6279–6294, Jun. 2024.
- [8] Y. Shen et al., "Design and implementation of mmWave surface wave enabled fluid antennas and experimental results for fluid antenna multiple access," arXiv preprint, arXiv:2405.09663, May 2024.
- [9] J. Zhang et al., "A novel pixel-based reconfigurable antenna applied in fluid antenna systems with high switching speed," *IEEE Open J. Antennas & Propag.*, vol. 6, no. 1, pp. 212-228, Feb. 2025.

- [10] L. Zhu and K.-K. Wong, "Historical review of fluid antenna and movable antenna," arXiv preprint, arXiv:2401.02362v2, 2024.
- [11] K.-K. Wong, "Transmitter CSI-free RIS-randomized CUMA for extreme massive connectivity," *IEEE Open J. Commun. Soc.*, vol. 5, pp. 6890– 6902. Oct. 2024.
- [12] B. Tang et al., "Fluid antenna enabling secret communications," IEEE Commun. Lett., vol. 27, no. 6, pp. 1491–1495, Apr. 2023.
- [13] H. Xu et al., "Capacity maximization for FAS-assisted multiple access channels," *IEEE Trans. Commun.*, doi:10.1109/TCOMM.2024.3516499, Dec. 2024.
- [14] Y. Chen, S. Li, Y. Hou, and X. Tao, "Energy-efficiency optimization for slow fluid antenna multiple access using mean-field game," *IEEE Wireless Commun. Lett.*, vol. 13, no. 4, pp. 915–918, Apr. 2024.
- [15] K.-K. Wong and K.-F. Tong, "Fluid antenna multiple access," *IEEE Trans. Wireless Commun.*, vol. 21, no. 7, pp. 4801–4815, Jul. 2022.
- [16] H. Xu et al., "Revisiting outage probability analysis for two-user fluid antenna multiple access system," *IEEE Trans. Wireless Commun.*, vol. 23, no. 8, pp. 9534–9548, Aug. 2024.
- [17] L. Tlebaldiyeva, S. Arzykulov, A. Dadlani, K. M. Rabie, and G. Nauryzbayev, "Exploring the performance of fluid antenna system (FAS)-aided B5G mmWave networks," in *Proc. IEEE Globecom*, pp. 7568–7573, Dec. 2023, Kuala Lumpur, Malaysia.
- [18] X. Lai et al., "FAS-assisted wireless powered communication systems," arXiv preprint, arXiv:2402.02159, 2024.
- [19] L. Tlebaldiyeva, S. Arzykulov, K. M. Rabie, X. Li, and G. Nauryzbayev, "Outage performance of fluid antenna system (FAS)-aided terahertz communication networks," in *Proc. IEEE Int. Conf. Commun. (ICC)*, pp. 1922–1927, May/Jun. 2023, Rome, Italy.
- [20] Y. Chen et al., "Joint beamforming and antenna design for near-field fluid antenna system," *IEEE Wireless Commun. Lett.*, vol. 14, no. 2, pp. 415–419, Feb. 2025.
- [21] L. Zhou et al., "Fluid antenna-assisted simultaneous wireless information and power transfer systems," arXiv preprint, arXiv:2407.11307, 2024.
- [22] K. Meng, C. Masouros, A. P. Petropulu, and L. Hanzo, "Cooperative ISAC networks: Opportunities and challenges," *IEEE Wireless Commun.*, vol. 32, no. 3, pp. 212–219, Jun. 2025.
- [23] F. Liu et al., "Integrated sensing and communications: Toward dual-functional wireless networks for 6G and beyond," IEEE J. Sel. Areas Commun., vol. 40, no. 6, pp. 1728–1767, Jun. 2022.
- [24] K. Meng, C. Masouros, K.-K. Wong, A. P. Petropulu, and L. Hanzo, "Integrated sensing and communication meets smart propagation engineering: Opportunities and challenges," *IEEE Network*, vol. 39, no. 2, pp. 278–285, Mar. 2025.
- [25] C. Wang et al., "Fluid antenna system liberating multiuser MIMO for ISAC via deep reinforcement learning," *IEEE Trans. Wireless Commun.*, vol. 23, no. 9, pp. 10879–10894, Sept. 2024.
- [26] F. R. Ghadi, K.-K. Wong, F. J. Lopez-Martinez, H. Shin, and L. Hanzo, "Performance analysis of FAS-aided NOMA-ISAC: A backscattering scenario," arXiv preprint, arXiv:2408.04724, 2024.